Optical and spectral properties of quantum domain walls in the generalized Wigner lattice

S. Fratini[1] and G. Rastelli[1,2]
[1]*Institut Néel-CNRS and Université Joseph Fourier, Boîte Postale 166, F-38042 Grenoble Cedex 9, France*
[2]*Istituto dei Sistemi Complessi, CNR-INFM, via dei Taurini 19, 00185 Roma, Italy*
(Received 17 January 2007; revised manuscript received 13 March 2007; published 4 May 2007)

We study the spectral properties of a system of electrons interacting through long-range Coulomb potential on a one-dimensional chain. When the interactions dominate over the electronic bandwidth, the charges arrange in an ordered configuration that minimizes the electrostatic energy, forming Hubbard's generalized Wigner lattice. In such strong-coupling limit, the low-energy excitations are quantum domain walls that behave as fractionalized charges and can be bound in excitonic pairs. Neglecting higher-order excitations, the system properties are well described by an effective Hamiltonian in the subspace with one pair of domain walls, which can be solved exactly. The optical conductivity $\sigma(\omega)$ and the spectral function $A(k,\omega)$ can be calculated analytically and reveal unique features of the unscreened Coulomb interactions that can be directly observed in experiments.

DOI: 10.1103/PhysRevB.75.195103 PACS number(s): 73.20.Qt, 78.20.Bh, 71.10.Fd, 73.20.Mf

I. INTRODUCTION

Quantum many-body systems often exhibit complex behavior, arising from the strong interactions between the individual degrees of freedom. In some cases, the exotic physical properties can be simply explained in terms of suitable renormalized collective excitations. Well-known examples are the charge-spin separation in the Luttinger liquid with gapless bosonic excitations,[1] solitons on a charge-density wave (CDW) condensate,[2] and fractional charges in quantum Hall systems.[3] Another system that exhibits emerging complex behavior is the generalized Wigner lattice (GWL), defined as the classical charge pattern that minimizes the Coulomb repulsion on a discrete lattice. The GWL was introduced by Hubbard[4] to explain the charge ordering observed in the TTF-TCNQ organic salts, and has since been invoked in several classes of narrow-band quasi-one-dimensional compounds.[5–7] Increasing the electron bandwidth smears the classical charge distribution and eventually drives the system toward a small amplitude charge-density wave.[8]

In the strongly interacting limit, where the bandwidth is much smaller than the electrostatic repulsive energy, the quantum charge distribution remains very close to the classical configuration. In this limit, the low-lying excitations are pairs of domain walls (kinks and antikinks) that carry fractional charge.[4,9,10] It follows that the low-energy properties of the system can be determined by solving the problem of two interacting domain walls, which is equivalent to the Coulomb problem on a one-dimensional chain. Since kinks and antikinks have opposite charges, the lowest-lying excitations of the GWL will be bound pairs, followed by a continuum of unbound domain walls. Restricting to the subspace with only one kink-antikink pair, the quantum melting of the GWL was estimated in Ref. 9 as the point where the gap in the excitation spectrum vanishes. The result is in agreement with previous variational estimates[8] as well as with more recent exact diagonalization data,[10] indicating that the single-pair approximation captures the essential physics of the GWL phase. On the other hand, it clearly breaks down close to the quantum melting transition, where a proliferation of domain walls is expected.

In this paper, we take advantage of the exact solution of the discrete Coulomb problem given in Refs. 11 and 12 to evaluate the optical conductivity of the generalized Wigner lattice at simple commensurate fillings $\rho=1/s$. The formation of excitons manifests through the emergence of a series of sharp peaks, followed by a strongly asymmetric absorption band due to the kink-antikink continuum, characterized by a sharp absorption edge. Remarkably, both the discrete peaks and the edge singularity are direct consequences of the long-range interactions among the electrons in the original model that disappear when the Coulomb interactions are replaced by short-range potentials.

An analogous formalism is used to calculate the spectral function $A(k,\omega)$. However, since the addition or removal of an electron to a GWL at filling $\rho=1/s$ is equivalent to the creation of s domain walls,[9] the single-pair approximation only applies to the special case $\rho=1/2$. The interactions being repulsive, because the domain walls have equal charge, the low-lying excitations in the spectral function are unbound scattering states, while antibound states appear as a set of dispersive quasiparticle peaks above the continuum.[13]

The paper is organized as follows. In Sec. II, we introduce the one-dimensional model for spinless fermions with long-range interactions and solve it in the narrow-band regime, restricting to the subspace with one pair of domain walls. In Secs. III and IV, we use this analytical solution to calculate, respectively, the optical conductivity and the single-particle spectral function. The results are briefly discussed in Sec. V in connection with existing experimental work.

II. MODEL AND SINGLE-PAIR APPROXIMATION

We consider the following Hamiltonian for fermions on a linear chain, interacting through long-range Coulomb forces:

$$H = -t\sum_i (c_i^\dagger c_{i+1} + c_i^\dagger c_{i-1}) + \frac{V}{2}\sum_{i\neq j} \frac{(n_i-\rho)(n_j-\rho)}{|i-j|}. \quad (1)$$

Here, t is the nearest-neighbor hopping amplitude and V sets the energy scale of the long-range repulsion, $V_m = V/|m|$.

$\{c_i^\dagger, c_i\}$ are, respectively, the fermionic creation and annihilation operators, $n_i = c_i^\dagger c_i$ is the occupation number at site i, and ρ is the average charge per site. The spin degrees of freedom are explicitly neglected, corresponding to the limit of large on-site repulsion U. The lattice parameter is set to unity.

Since we are interested in the strong-coupling regime, it is useful to start by describing the classical solution, obtained for $t=0$. At simple commensurate fillings $\rho = 1/s$, the ground state takes one of the s equivalent configurations that minimize the electrostatic energy, with one electron on every sth site.[14] The excited configurations of lowest energy correspond to the inclusion of a domain with a different (shifted) ground state, delimited by a kink and an antikink.[9] The energy cost to form a classical domain of finite length sd (d is the number of perturbed unit cells) can be calculated as

$$\Delta_s(d) = \sum_{p=1}^{d} \sum_{m=p}^{\infty} (V_{sm+1} + V_{sm-1} - 2V_{sm}). \tag{2}$$

It defines an effective interaction between the domain walls and can be evaluated exactly in terms of digamma functions. However, a very good approximation is obtained by expanding in powers of $1/sd$ and keeping only the leading term

$$\Delta_s(d) \simeq \Sigma_s - \frac{V}{s^2}\frac{1}{sd}. \tag{3}$$

The above expression can be directly interpreted as the Coulomb attraction between two defects of charge $\pm 1/s$ at distance sd, with $\Sigma_s = \frac{V}{s}\left[1 - \frac{\pi}{s}\cot\left(\frac{\pi}{s}\right)\right]$, the energy cost for creating two isolated defects at infinite distance. The approximate result [Eq. (3)] is quite accurate even at short distances.[15] Unless otherwise specified, we shall neglect the higher-order terms (dipolar and multipolar interactions) in the following.

According to the above discussion, the gap in the excitation spectrum is given classically by $\Delta_s(1)$. Actually, this can be viewed as the effective coupling parameter of the model that determines the stability of the classical charge pattern against quantum fluctuations, so that the melting of the GWL is expected when $t \gtrsim \Delta_s(1)$.[8] Since the gap scales as $\sim V/s^3 \sim Vn^3$, we see that for any finite value of the hopping integral t, the formation of a GWL becomes unfavorable at very low fillings. In this case, an ordinary Wigner crystal phase is more likely realized, where the electron wave functions are spread on length scales much larger than the lattice spacing,[8] and for which the usual continuum approach would be more suitable. A similar argument shows that the GWL phase is unfavored when moving away from the simple commensurate fillings $\rho = 1/s$. Indeed, at generic rational fillings $\rho = r/s$, it is easily shown that the gap still scales as $\sim V/s^3$ (i.e., it is governed by the periodicity s of the classical pattern), which can be arbitrarily small regardless of the value of ρ.[16] In the following, we shall therefore restrict to the special fillings $\rho = 1/s$, where the physics of the GWL is more relevant, leaving the study of the continuum Wigner crystal phase for future work.

Let us denote $|m,d\rangle$ the classical state corresponding to a kink-antikink pair of length sd, with center of mass at m. The total two-body wave function in the quantum case can be written as

$$\Psi_{K,\lambda} = \sqrt{\frac{s}{2L}} \sum_{m=-L/s}^{L/s} \sum_{d=-L/2s}^{L/2s} e^{iKm} \varphi_{K,\lambda}(d) |m,d\rangle, \tag{4}$$

where the center of mass of the pair moves freely with momentum K, while the radial part obeys the following discrete Schrödinger equation:[9,17]

$$-2t(K)[\varphi(d+1) + \varphi(d-1)] + \left(\Sigma_s - \frac{V/s^3}{d} - E\right)\varphi(d) = 0, \tag{5}$$

with the boundary condition $\varphi(0)=0$. The factor $t(K) = t\cos(Ks/2)$ reflects the fact that at each electron hopping event, the center of mass of the defect pair moves by $\pm s/2$ lattice sites. The discrete hydrogen problem on the semi-infinite chain admits an exact analytical solution[11,12] in terms of Gauss-hypergeometric functions (or, equivalently, of incomplete beta functions). The excitation spectrum consists, as in the ordinary hydrogen atom, of an *infinite* series of bound states (kink-antikink excitons), followed by a continuum of scattering states. Observing that the two subspaces of different polarity $d>0$ and $d<0$ is disconnected when only nearest-neighbor electron hopping is allowed,[10] the solution of the Coulomb problem [Eq. (5)] on the infinite chain is obtained straightforwardly by constructing combinations of even or odd parity of the wave functions on the half-chain. We now consider separately the bound and unbound solutions of Eq. (5).

A. Domain-wall excitons

The bound states have energies

$$E_{K,n} = \Sigma_s - \sqrt{16t(K)^2 + \left[\frac{V}{s^3(n+1)}\right]^2}, \tag{6}$$

with $n = 0, 1, 2, \ldots, \infty$. Introducing the parameter $\sinh(k_n) = V/[4s^3 t(K)(n+1)]$, the normalized radial wave functions can be written as

$$\varphi_{K,n}(d) = A_n d e^{-k_n d} {}_2F_1(1-d, -n; 2; 1-e^{2k_n}), \tag{7}$$

where ${}_2F_1$ is one of the Gauss-hypergeometric functions and A_n is a normalization constant:

$$A_n = 2\sinh(k_n)\sqrt{\tanh(k_n)}e^{-nk_n}. \tag{8}$$

The exciton radius, defined as $r_n = \Sigma_{d=1}^{\infty} d|\varphi_{K,n}(d)|^2$, can also be evaluated as[12]

$$r_n = (n+1)\frac{2+\cosh(2k_n)}{\sinh(2k_n)}. \tag{9}$$

In the strong-coupling regime, $r_n \approx (n+1)$ and the first bound state ($n=0$) is strongly localized on one lattice spacing. At large quantum numbers, the radius increases as $r_n \simeq (6s^3 t/V)(n+1)^2$ approaching the free scattering states.

B. Kink-antikink continuum

The energy of the scattering states is given by the sum of the energies of the individual domain walls, with k the relative momentum of the two-body system

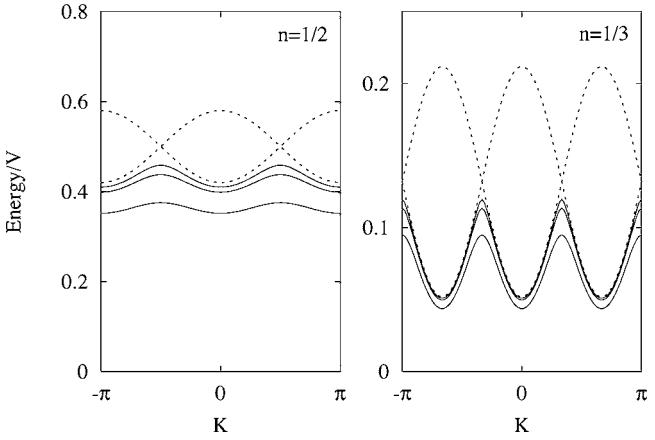

FIG. 1. Excitation spectrum vs center-of-mass momentum K in the single-pair subspace for $t/V=0.02$ at fillings $\rho=1/2$ (left) and $\rho=1/3$ (right). The full lines correspond to the three lowest bound states, while the dashed lines indicate the boundaries of the kink-antikink continuum.

$$E_{K,k} = \Sigma_s - 2t[\cos(Ks/2+k) + \cos(Ks/2-k)]. \quad (10)$$

The corresponding wave function is[12]

$$\varphi_{K,k}(d) = B^{-1}(k) d e^{ikd}\, {}_2F_1[1-d, 1-i\eta(k); 2; 1-e^{-2ik}], \quad (11)$$

where $\eta(k)=V/[2s^3 t(K)\sin k]$. The normalization factor is determined by the asymptotic behavior at large d and is given by

$$B^{-2}(k) = \frac{4s}{L}\frac{\pi\eta(k)}{\sinh[\pi\eta(k)]}\sin^2(k) e^{-(2k-\pi)\eta(k)} \quad (12)$$

in the case of an open chain of length $L/2s$.

The excitation spectrum is illustrated in Fig. 1 for $t/V=0.02$ at fillings $\rho=1/2$ and $\rho=1/3$. The gap in the excitation spectrum is obtained from Eq. (6) setting $K=0$ and $n=0$:

$$\Delta_s^{opt} = \Sigma_s - 4t\sqrt{1+\left(\frac{V}{4ts^3}\right)^2}. \quad (13)$$

This value is lower than the classical value $\Delta_s(1)$ because of the energy gain due to charge delocalization. The condition $\Delta_s^{opt} \to 0$ can be used to locate the melting of the GWL as the region where charge defects are expected to proliferate.[9] For the quarter-filled case $s=2$, the estimate $t/V \simeq 0.12$ is in good agreement with the numerical results of Ref. 10.

III. OPTICAL CONDUCTIVITY

The finite frequency absorption at $T=0$ can be expressed in terms of the current-current correlation function through the Kubo formula

$$\sigma(\omega) = \frac{1}{L\omega}\,\mathrm{Im}\sum_{K,\lambda}\frac{|\langle\Psi_{K,\lambda}|\hat{j}|\psi_{GS}\rangle|^2}{\omega - E_{K,\lambda} + i0^+}, \quad (14)$$

where the sum runs over all eigenstates, and the ground-state energy is set to 0. For nearest-neighbor hopping, the current operator on the lattice is defined as $\hat{j}=it\Sigma_i(c_i^+ c_{i+1} - c_{i+1}^+ c_i)$. The above dimensionless expression should be multiplied by a prefactor $\sigma_0=e^2a^2/\hbar v$ to restore the proper units, where a is the intersite distance on the chain and v is the volume of the unit cell.

Approximating $|\psi_{GS}\rangle$ in the GWL phase at fillings $\rho=1/s$ with the classical state $|\psi_\infty\rangle=\Pi_i c_{si}^\dagger|0\rangle$, we see that the effect of the operator $\hat{j}$ is to create kink-antikink pairs of length $d=\pm 1$ at any of the m possible sites. The matrix elements with the single-pair states of Eq. (4) are thus given, in terms of the eigenfunctions of the semi-infinite chain, as

$$|\langle\psi_\infty|\hat{j}|\Psi_{K,\lambda}\rangle|^2 = t^2\frac{L}{s}\delta_{K,0}|\varphi_{K,\lambda}(1)|^2. \quad (15)$$

A. Coulomb potential

The optical absorption can be divided into two parts $\sigma=\sigma_{exc}+\sigma_{sc}$, which represent, respectively, the sharp transitions from the ground state to the excitonic states and an absorption band due to transitions to the kink-antikink continuum. The corresponding energies are obtained from Eqs. (6) and (10) by setting $K=0$. The excitonic part is an infinite series of delta function peaks

$$\sigma_{exc} = \sum_n \frac{\pi t^2}{sE_{0,n}}|\varphi_{0,n}(1)|^2\delta(\omega - E_{0,n}), \quad (16)$$

where the spectral weights are given by Eqs. (7) and (8) above, making use of the property ${}_2F_1=1$ at $d=1$. Setting $k(\omega)=\arccos[-(\omega-\Sigma_s)/4t]$ and converting the sum over states in Eq. (14) into an integral, we obtain the following analytical expression for the continuous absorption band:

$$\sigma_{sc}(\omega) = \left(\frac{\pi V}{4s^4\omega}\right)\frac{e^{-(V/2s^3t)[k(\omega)/\sin k(\omega)]}}{1-e^{-(V/2s^3t)[\pi/\sin k(\omega)]}}. \quad (17)$$

Since we are assuming $t \lesssim V/s^3$, the denominator can be set equal to 1 up to exponentially small corrections (these become important close to the melting of the GWL, where anyway the single-pair approximation breaks down).

It should be noted that, even though the assumption $t \lesssim V/s^3$ is needed to justify the restriction to the single-pair subspace, in practice, the above expression is obtained from the exact solution of the Coulomb problem to all orders in t/V. Indeed, the presence of an essential singularity in Eq. (17) shows that this result cannot be obtained from a perturbation expansion in t/V. It reflects the fact that the delocalized nature of the scattering states is lost for any finite truncation of the expansion in t/V.

The optical absorption determined above is illustrated in Fig. 2(a) and agrees remarkably well with the exact diagonalization results of Ref. 10. The main discrepancy is a shift in the position of the first excitonic peak that can be entirely ascribed to the use of the pure Coulomb potential in Eq. (3) instead of the full potential in Eq. (2). A transfer of spectral weight from the excitons to the kink-antikink continuum takes place as t/V increases, as shown in Fig. 2(b), where we have plotted the quantities $\int d\omega\sigma_{exc}(\omega)/\int d\omega\sigma(\omega)$ and

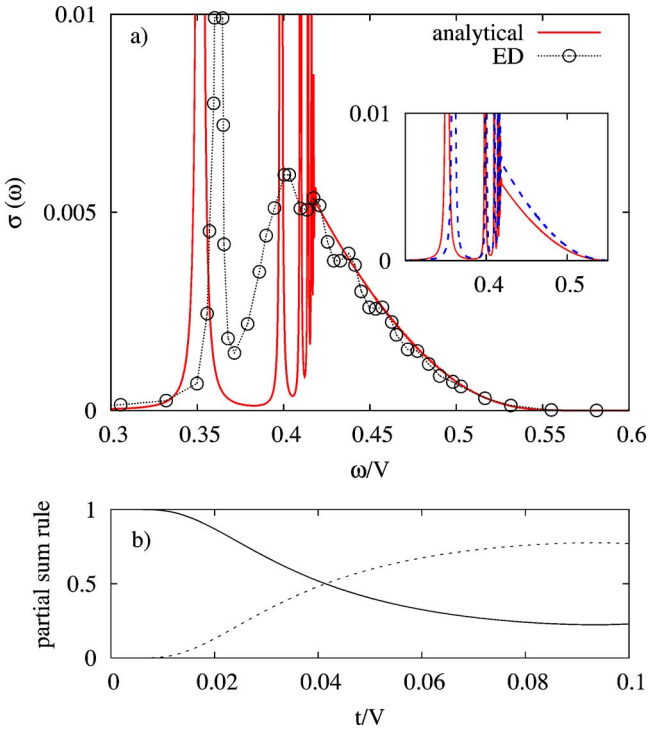

FIG. 2. (Color online) (a) Optical conductivity of the generalized Wigner lattice in the single-pair approximation as given by Eqs. (16) and (17) at $\rho=1/2$ and $t/V=0.02$. A finite broadening has been introduced for graphical purposes. The open circles are the exact diagonalization data of Ref. 10. In the inset, the same curve is compared with the result obtained with the full potential of Eq. (2) (dashed lines). (b) Fraction of the spectral weight carried by the excitons (full lines) and the kink-antikink continuum (dashed line), respectively.

$\int d\omega\sigma_{sc}(\omega)/\int d\omega\sigma(\omega)$. Note that formulas (16) and (17) obey the following property that derives from the closure relation of the eigenstates of Eq. (5):

$$\langle\omega\rangle = \int d\omega\sigma(\omega)\omega = \pi t^2/s. \tag{18}$$

This relation shows that the "average" absorption frequency is independent of the interaction potential and can be used to measure directly the value of the hopping integral in an optical-absorption experiment.

In the above derivation, it was assumed that the potential follows a pure Coulomb law, Eq. (3), which allowed us to obtain explicit analytical formulas for the optical absorption. However, the discrete Schrödinger equation (5) with the exact potential $\Delta_s(d)$ of Eq. (2) can be solved to arbitrary accuracy with small numerical effort. The result is presented in the inset of Fig. 2(a). We see that the analytical expression (17) agrees quite well with the numerical result. Discrepancies arise at very small values of t/V, where the excitons become localized on very short length scales, which is where the potential $\Delta_s(d)$ sensibly deviates from the Coulomb law.

Note that an expression similar to Eq. (17) was derived by Gallinar[18] in the half-filled case $\rho=1$ for electrons with spin, in the limit of a large on-site repulsion U. In that case, the lowest-lying excitations correspond to pairs of doubly occupied and/or empty sites.[19] The energy cost for creating such pairs is set by U, while the long-range tail of the Coulomb potential acts to bind the opposite charges together.[20] Similar effects have also been discussed in the context of conjugated polymers, in which case, the energy scale of an electron-hole exciton is set by the Peierls dimerization gap[21] (see also Ref. 19).

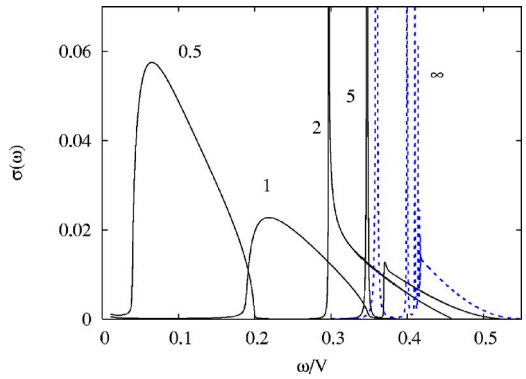

FIG. 3. (Color online) Optical absorption for a screened potential at $\rho=1/2$ and $t/V=0.02$. The labels indicate the value of the screening length ℓ. The dashed line corresponds to the unscreened Coulomb potential.

B. Screened potentials

The characteristic optical line shape [Eq. (17)] ultimately follows from the long-range nature of the Coulomb potential. Indeed, although the energies of the scattering states are given by the noninteracting expression (10), their wave functions strongly differ from the free plane waves especially at short distances (the scattering states are required to be orthogonal to the bound states). This is reflected in the optical absorption, which involves the wave function precisely at $d=1$, where the condition of orthogonality with the excitonic states is most stringent. To illustrate this issue, we have considered the case of a screened potential $V/d \to V\exp(-d/\ell)/d$. This potential is convex and ensures the stability of the classical configuration considered here,[4] which is preferable to the case of arbitrarily truncated Coulomb interactions, for which the ground state is not always univocally determined.

The results obtained for generic values of the screening length are reported in Fig. 3 at filling $\rho=1/2$, for $t/V=0.02$. Upon reducing the screening length, the optical absorption shifts to lower frequencies, the discontinuity at the absorption edge is smoothened, the asymmetry of the line shape becomes less marked, and the excitonic peaks progressively disappear (below a critical value, no bound states are possible and $\sigma_{exc}=0$). In the limit $\ell\to 0$, a truncated nearest-neighbor potential is recovered. In that case, the effective interaction $\Delta(d)=Ve^{-1/\ell}\equiv V_1$ is constant for all d and the scattering states reduce to free-particle states. The corresponding current-current correlation function has a semicircular shape and the resulting absorption band is

$$\sigma_{nn}(\omega) = \frac{t}{2\omega}\sqrt{1-\left(\frac{\omega-V_1}{4t}\right)^2}. \tag{19}$$

To conclude this section, let us stress that the experimental observation of an edge singularity in the absorption line shape, as shown in Fig. 2(a), can be taken as a signature of the importance of long-range electron-electron interactions in a given material and calls for theoretical models that go beyond the intersite repulsion term usually considered.[22]

IV. SPECTRAL FUNCTION AT QUARTER FILLING

In a photoemission experiment, an electron is added or removed from the system in a sudden process that is described by the single-particle spectral function $A(q,\omega) = -\frac{1}{\pi}\,\mathrm{Im}\,G(q,\omega)$. In the spirit of the strong-coupling approach presented in the preceding section, adding an electron to the classical configuration at $\rho = 1/s$ creates s kinks of charge $1/s$. Analogously, removing an electron creates s antikinks of negative charge $-1/s$. In the special case $s=2$, two defects are created and the problem becomes equivalent to the one treated previously, albeit with repulsive interactions (the analogy is no longer true for larger values of s, where the creation or removal of an electron takes the system away from the single-pair subspace).

Classically, since the interaction potential is repulsive, the state of lowest energy in the system with one particle added (removed) corresponds to configurations where the two kinks (antikinks) are far apart. The creation energy of each kink is $\Sigma_2/2 = V/4$ [see Eq. (3)].

In the quantum case, we can write the one-dimensional Schrödinger equation for the two-body problem, which is formally identical to the one presented in Sec. II, except for a change of sign in the interaction potential. This results in a symmetrically reflected excitation spectrum: the low-energy part now corresponds to the domain-wall continuum, while the discrete levels are moved to higher energies. The formation of such *antibound* states is due to the long-range nature of the repulsive potential, as for the excitonic states encountered previously.

The spectral function for $\omega > 0$, which describes the inverse photoemission processes, can be calculated as

$$A(q,\omega) = \sum_{K,\lambda} |\langle \Psi_{K,\lambda}|c_q^+|\psi_{GS}\rangle|^2 \delta(\omega - E_{K,\lambda}), \tag{20}$$

where $c_q^+ = \frac{1}{\sqrt{L}}\Sigma_m e^{iqm} c_m^+$ and $|\Psi_{K,\lambda}\rangle$ are the solutions of the repulsive Schrödinger equation (5). An analogous formula holds at $\omega < 0$, with $A(q,-\omega) = A(q,\omega)$. Replacing as usual the ground state with the classical configuration at $t=0$ enforces the constraint that electrons can only be created on the unoccupied sites. The resulting expression for the spectral function is

$$A(q,\omega) = \frac{1}{2}\sum_{\lambda} |\varphi_{q,\lambda}|^2 \delta(\omega - E_{q,\lambda}), \tag{21}$$

where the sum runs over both the continuous spectrum ($\lambda \equiv k$) and the discrete antibound states ($\lambda \equiv n$), whose energies are given by Eqs. (10) and (6), respectively. We reproduce the latter here (the sign of the square-root term reflects the repulsive nature of the interactions) as

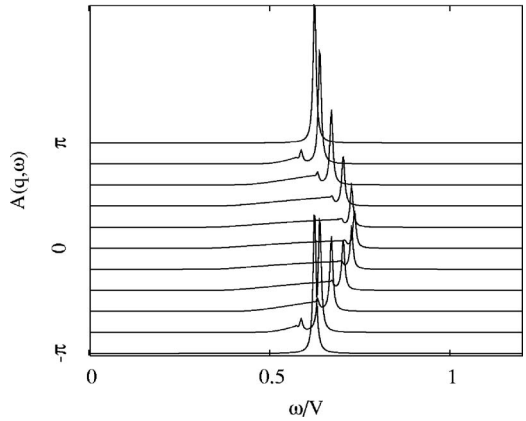

FIG. 4. Spectral function $A(q,\omega)$ for $s=2$ and $t/V=0.05$. The different curves correspond to different values of q, as indicated on the left axis. Two dispersive antibound states are visible above the kink-antikink continuum. A finite Lorentzian broadening has been introduced for clarity.

$$E_{q,n} = \frac{V}{2} + \sqrt{16t^2\cos^2(q) + \left[\frac{V}{8(n+1)}\right]^2}. \tag{22}$$

The results are reported in Fig. 4. The width of the continuous spectrum is modulated by q and vanishes at $q = \pm\pi$. The first two antibound states are clearly observable as well defined quasiparticle peaks in $A(q,\omega)$ that follow the roughly sinusoidal dispersion relations [Eq. (22)].

V. DISCUSSION AND CONCLUSIONS

In this work, we have examined the spectral properties of spinless electrons interacting through the long-range Coulomb potential on a one-dimensional lattice, which constitutes a minimal model to address the effects of electronic correlations in narrow-band solids, away from the most studied half-filled case. In the strongly interacting regime, the charges form a generalized Wigner lattice, whose elementary excitations are fractionally charged domain walls, themselves interacting through long-range forces. Taking advantage of the exact solution of the Coulomb problem on a one-dimensional chain, we have derived an analytical expression for the optical conductivity at simple commensurate fillings $\rho = 1/s$, as well as for the single-particle spectral function in the special case $\rho = 1/2$. Both are in good agreement with the available exact diagonalization data at $\rho = 1/2$.[10,13]

The sharp peaks emerging in the optical conductivity, signaling the formation of domain-wall excitons, the asymmetric line shape of the absorption continuum, with its characteristic edge singularity, as well as the sharp quasiparticle peaks in the single-particle spectral function, are all robust features that follow from the long-range nature of the Coulomb potential and that are lost in models with strongly screened or truncated interactions. These features should be clearly observable in experiments, allowing to address the relevance of long-range interactions in the charge-ordered insulating phases of narrow-band one-dimensional systems.

As an example, the midinfrared optical-absorption band recently measured[23] in the organic quarter-filled ($\rho=1/2$) salt $(DI\text{-}DCNQI)_2Ag$—a prototypical system exhibiting Wigner crystal ordering[5]—resembles very closely the theoretical spectra obtained from Eqs. (16) and (17), and a satisfactory fit can be obtained with physically sound parameters ($V=1.1$ eV and $t=80$ meV). Absorption shapes similar to the ones presented in this work have also been reported in other classes of organic compounds, such as DBTSF-$TCNQF_4$, TTF-TCNQ,[24] and $Cs_2(TCNQ)_3$,[25] corresponding, respectively, to $\rho=1$, $\rho\simeq 1/2$, and $\rho=1/3$, whose detailed analysis is postponed to future work.

ACKNOWLEDGMENTS

One of the authors (G.R.) was funded by the Swiss-Italian Foundation "Angelo Della Riccia." S.F. gratefully acknowledges enlightening discussions with D. Baeriswyl.

[1] J. Voit, Rep. Prog. Phys. **57**, 977 (1994).
[2] M. J. Rice, A. R. Bishop, J. A. Krumhans, and S. E. Trullinger, Phys. Rev. Lett. **36**, 432 (1976).
[3] R. B. Laughlin, Rev. Mod. Phys. **71**, 863 (1999).
[4] J. Hubbard, Phys. Rev. B **17**, 494 (1978).
[5] K. Hiraki and K. Kanoda, Phys. Rev. Lett. **80**, 4737 (1998); T. Itou, K. Kanoda, K. Murata, T. Matsumoto, K. Hiraki, and T. Takahashi, *ibid.* **93**, 216408 (2004).
[6] P. Abbamonte *et al.*, Nature (London) **431**, 1081 (2004); A. Rusydi, P. Abbamonte, H. Eisaki, Y. Fujimaki, G. Blumberg, S. Uchida, and G. A. Sawatzky, Phys. Rev. Lett. **97**, 016403 (2006).
[7] P. Horsch, M. Sofin, M. Mayr, and M. Jansen, Phys. Rev. Lett. **94**, 076403 (2005).
[8] B. Valenzuela, S. Fratini, and D. Baeriswyl, Phys. Rev. B **68**, 045112 (2003).
[9] S. Fratini, B. Valenzuela, and D. Baeriswyl, Synth. Met. **141**, 193 (2004).
[10] M. Mayr and P. Horsch, Phys. Rev. B **73**, 195103 (2006).
[11] J.-P. Gallinar, Phys. Lett. **103A**, 72 (1984).
[12] A. A. Kvitsinski, J. Phys. A **25**, 65 (1992).
[13] M. Daghofer and P. Horsch, Phys. Rev. B **75**, 125116 (2007).
[14] The electrostatic energy *per particle* in the classical state is

$$\mathcal{E}_{GS}=\frac{s-1}{s^2}\gamma+\frac{2}{s^3}\sum_{m=1}^{s-1} m\left[\Psi\left(\frac{m}{s}\right)+\frac{\pi}{s}\cot\left(\frac{\pi m}{s}\right)\right],$$

where γ is the Euler constant and $\Psi(x)$ is the digamma function.
[15] The effective potential can be evaluated as

$$\Delta_s(d)=\Sigma_s+\frac{V}{s^2}[\Psi(d-1/s)-\Psi(d+1/s)]$$

$$+V\frac{d}{s}[2\Psi(d)-\Psi(d+1/s)-\Psi(d-1/s)].$$

The largest discrepancy occurs for $s=2$ and $d=1$, where the above expression gives $\Delta_2(1)\simeq 0.386$ V while the value for the pure Coulomb law is 0.375 V.
[16] V. Slavin, Phys. Status Solidi B **242**, 2033 (2005).
[17] W. Barford, Phys. Rev. B **65**, 205118 (2002).
[18] J.-P. Gallinar, Phys. Rev. B **48**, 5013 (1993).
[19] F. B. Gallagher and S. Mazumdar, Phys. Rev. B **56**, 15025 (1997).
[20] In the antiferromagnetic phase, the problem is formally equivalent to the one treated here [set $x=1$ in Eq. (3.1) of Ref. 16]. For more general magnetic arrangements, the excitation spectrum must be modified to account for the probability of finding neighboring sites with opposite spins, leading to a more complex scenario for the optical absorption.
[21] S. Abe, J. Phys. Soc. Jpn. **58**, 62 (1989).
[22] H. Seo, J. Merino, H. Yoshioka, and M. Ogata, J. Phys. Soc. Jpn. **75**, 051009 (2006).
[23] K. Yamamoto, T. Yamamoto, K. Yakushi, C. Pecile, and M. Meneghetti, Phys. Rev. B **71**, 045118 (2005).
[24] C. S. Jacobsen, I. Johannsen, and K. Bechgaard, Phys. Rev. Lett. **53**, 194 (1984).
[25] K. D. Cummings, D. B. Tanner, and J. S. Miller, Phys. Rev. B **24**, 4142 (1981).